2.4 Higgs Boson Searches and Properties

2.4.1 Introduction

Despite the extraordinary success of the Standard Model (SM) in describing particle physics up to the highest energy available today, the mechanism responsible for electroweak symmetry breaking (EWSB) has yet to be determined. In particular, the Higgs boson [33, 34, 35] predicted in the minimal Standard Model and the theoretically attractive Supersymmetric (SUSY) Grand Unified Theory (GUT) extensions thereof have yet to be observed. If EWSB does indeed derive from nonzero vacuum expectation values for elementary scalar Higgs fields, then one of the primary goals of constructing future colliders must be to *completely* delineate the Higgs boson sector. In particular, it will be crucial to discover all of the physical Higgs bosons and determine their masses, widths and couplings. Conversely, if a fundamental Higgs boson does not exist, it is essential to demonstrate this unambiguously.

The EWSB mechanism in the Standard Model is phenomenologically characterized by a single Higgs boson (h_{SM}) in the physical particle spectrum. The mass of the h_{SM} is undetermined by the theory, but its couplings to fermions and vector bosons are completely determined. In SUSY theories, there are two Higgs doublets with vacuum expectation values v_1, v_2. These contribute mass terms for the gauge bosons proportional to $(v_1^2 + v_2^2)$, masses for down-type fermions proportional to v_1, and masses for up-type fermions proportional to v_2. In the Minimal Supersymmetric Standard Model (MSSM) [36, 37] these two doublets give rise to five physical Higgs bosons: h^0, the lighter of the two CP-even states; H^0, the heavier CP-even state; the CP-odd A^0 boson, and a pair of charged bosons $H^\pm$. The mass of the minimal SM Higgs boson is unspecified, but in the MSSM, there are tree-level relations which determine the spectrum of masses in terms of one of the boson masses (e.g., the mass of the A^0) and the ratio of the vacuum expectation values, v_2/v_1. The CP-even and CP-odd neutral Higgs bosons have nontrivial mixing angles α and β, respectively, which affect their couplings and decays. In particular, $v_2/v_1 = \tan\beta$. Both masses and couplings receive further radiative corrections which are functions of the SUSY Higgs mass parameter, μ, the scale of mass at which SUSY is broken, M_{SUSY}, the mass of the top quark, and the A_i parameters of the soft supersymmetry-breaking interaction. More general models of the Higgs sector, which also include electroweak singlets, are also possible in SUSY theories. Finally in non-supersymmetric models with two Higgs doublets (2HDM), the Higgs bosons may have mixed CP character.

Supersymmetry has exciting implications for the discovery potential of the Higgs bosons that it predicts. In the MSSM, considering renormalization group improved radiative corrections and assuming $m_t = 180$ GeV with the stop mass less than 1 TeV, the lightest Higgs boson must have mass $M_{h^0} \lesssim 130$ GeV. An even more sweeping statement can be made [38] that $M_{h^0} \lesssim 150$ GeV for *any* SUSY theory with a grand unification at high energy which includes the elementary Higgs fields.

2.4.2 Present and Future Limits

The best direct limits on the SM Higgs boson come from searches at LEP, with the present limit [39] being $M_{h_{SM}} > 65.2$ GeV at 95% confidence level (C.L.). These limits can also be interpreted in the framework of the MSSM to exclude the lightest SUSY Higgs with mass less than approximately 45 GeV. Electroweak radiative corrections including the top quark and the Higgs boson affect precision electroweak measurements, and global fits [40] using data from LEP, SLC, the Tevatron, and neutrino scattering give the relatively weak limit implying that $M_{h_{SM}} < 300$ GeV (95% C.L.).

LEP2

The limit on the Higgs boson mass will be improved in the near future with the operation of LEP2. With an integrated luminosity of 150 pb^{-1} in each of the four LEP detectors, expected from one year of running at design luminosity, the 5σ discovery reach can be increased [41] to about 95 GeV with running at center-of-mass energies of 192 GeV scheduled for 1997. At the same energy and luminosity, the process $e^+e^- \to hA$ can be discovered (excluded) at a cross section of 65 (30) fb, when supersymmetric decay channels are closed. The resultant exclusion region in the MSSM parameter space can be found in Fig. 2.13. The possibility of running at 205 GeV, which would result in an extension of limits close to the MSSM bound, is currently being investigated.

Upgraded Tevatron

The associated production of a Higgs boson and a W or Z boson, with the Higgs decaying to $b\overline{b}$ and the W or Z decaying leptonically, is a possible way to detect the Higgs in the mass range 60–130 GeV, at a high luminosity Tevatron collider [30]. The Higgs decay gives rise to 2 jets, thus one will use b tagging to reduce the large $W + 2$ jet background. It appears that the present b tagging capability at CDF is more than adequate to reduce this background (at moderate Run II luminosities, e.g., $10^{32}\times$ cm^{-2} sec^{-1}, 1 TeV $\times$ 1 TeV) if this capability is extended to larger rapidities (as is planned in Run II for both CDF and D0). After b tagging, the largest background at Higgs masses below 100 GeV is QCD production of $W + b\overline{b}$ and top backgrounds for masses above 100 GeV. Figure 2.12 shows the dijet mass distribution for the sum of all these backgrounds, plus the $W + H$ signal for 10 fb^{-1}. An observation of the Higgs for masses below 100 GeV is possible after the Main Injector upgrade, and is within reach of the present Run II accelerator after several years of data-taking. For higher mass Higgs bosons, these statistics are too low; one would need about 25 fb^{-1} to observe the 120 GeV Higgs. This study assumed an approximate 20% improvement in dijet mass resolution obtained from applying a clustering algorithm that reduces the effect of gluon radiation at large angles to the jet. This dijet mass resolution and jet clustering is crucial in seeing the Higgs. It has been argued that the $h \to \tau^+\tau^-$ and $Z \to \nu\overline{\nu}$ channels can be used to improve these results [43].

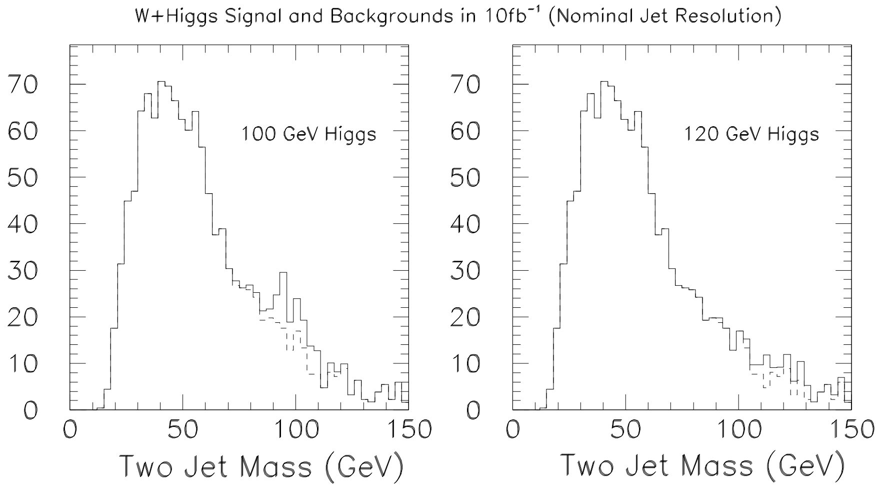

Figure 2.12: The signal plus background mass distributions for the WH process with 10 fb^{-1} of data at 2 TeV. The solid line is signal+background, the dashed line the sum of all backgrounds.

Large Hadron Collider

At the Large Hadron Collider (LHC), detection of the SM h_{SM} is possible through the process $gg \to h_{SM} \to \gamma\gamma$ for $M_{h_{SM}} < 150$ GeV and through $gg \to h_{SM} \to ZZ^{(*)} \to 4\ell$ for $M_{h_{SM}} > 130$ GeV. A heavy h_{SM} is also detectable in the reaction $WW \to h_{SM}$, with the Higgs decaying to ZZ and also, possibly, to WW. The $\gamma\gamma$ channel that is crucial for a light h_{SM} demands an excellent electromagnetic calorimeter, and much attention has been devoted to this in the LHC detector designs. For $M_{h_{SM}} < 120$ GeV, it will also be possible to detect $t\bar{t}h_{SM}$ and (possibly) Wh_{SM} with $h_{SM} \to b\bar{b}$, provided that the high b-tagging efficiency and purity projections are realized. Detection of the h_{SM} in the intermediate mass region when $M_{h_{SM}} < 2M_W$ generally requires accumulating data for at least a year when the LHC is run at full luminosity. This should be contrasted with e^+e^- collisions, where the $e^+e^- \to Zh_{SM}$ mode will allow detection in the same mass region in a matter of a few hours, assuming full instantaneous luminosity.

In the case of the MSSM for large M_{A^0}, the h^0 is similar to the Standard Model Higgs h_{SM}. As for the h_{SM}, the h^0 is straightforward to detect at an e^+e^- collider. On the other hand, the H^0 and A^0 do not resemble the Standard Model Higgs boson, and so one must separately consider their production process. We will show below that the observability of H^0 and A^0 at an e^+e^- collider depends only on the beam energy: for $\sqrt{s} > 2M_{A^0} - 20$ GeV, these particles are found in the reaction $e^+e^- \to Z^* \to H^0A^0$.

The story at the LHC is much more complex. The reactions which can be used to detect the Higgs particles of the MSSM, and their limits of applicability in parameter space, are displayed in Fig. 2.13 [35]. This figure represents the limit of the LHC capability, summing the results of two detectors in a multi-year run at design luminosity. For values of $M_A > 200$ GeV, the LHC can detect the H^0 and A^0 only in certain specific decay channels, shown in the figure, whose availability depends on the value of $\tan\beta$. Since this figure summarizes a great deal of analysis, we must point out at least a few of the assumptions which are used. The channel $A^0, H^0 \to \tau^+\tau^-$ can be used only when the branching ratio to τ is enhanced by a large value of $\tan\beta$. For small $\tan\beta$, modes with $b\bar{b}$ or $t\bar{t}$ in the final states require b tagging capabilities that will be challenging in the detection environment of the LHC. In addition, it should be noted that the process $A^0, H^0 \to t\bar{t}$ has so far been studied only at the level of the comparison of cross sections for signal and background, and that, since the signal is 2–10% of the background, an excellent knowledge of the $gg \to t\bar{t}$ cross section is required. Finally, though the h^0 should be detected for the generic situation illustrated in Fig. 2.13, there are regions of the full parameter space of the MSSM where the h^0 would not be observed [42]. Thus, it is unlikely that the whole MSSM Higgs spectrum would be observed at the LHC, and it is not possible to rule out the MSSM if none of its Higgs bosons are seen at the LHC.

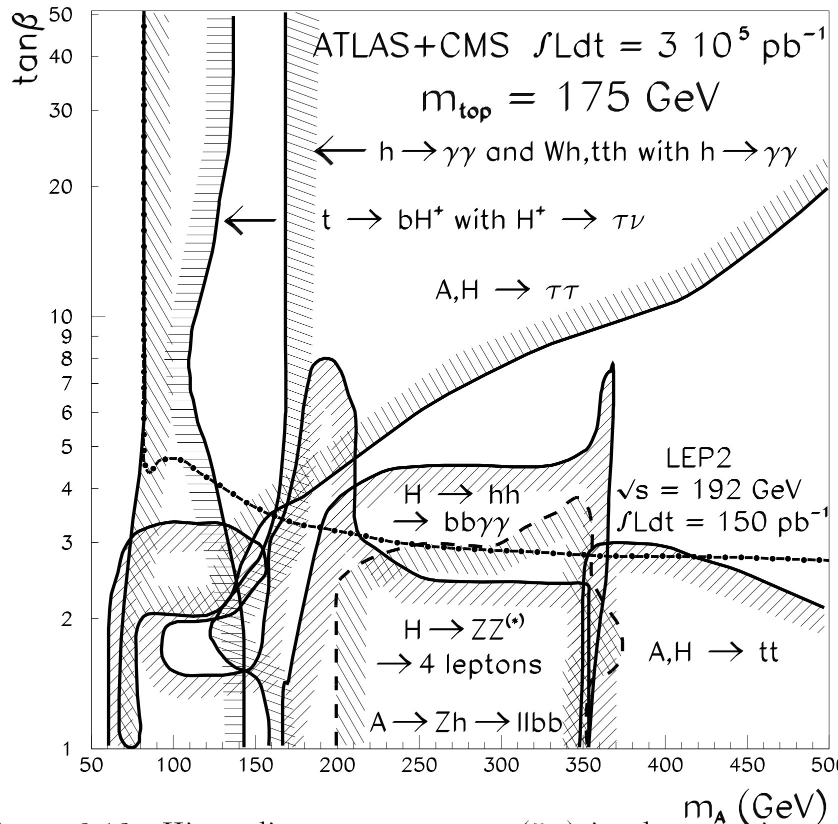

Figure 2.13: Higgs discovery contours (5σ) in the generic parameter space of the MSSM for ATLAS+CMS at the LHC, for a multi-year run at design luminosity, 300 fb^{-1} per detector, from [35]. Renormalization group improved radiative corrections are included for M_{h^0} and M_{H^0}, assuming $m_{\tilde{t}} = 1$ TeV and no squark mixing.

2.4.3 Standard Model Higgs

The main production processes for the SM Higgs in e^+e^- annihilation are $e^+e^- \rightarrow ZH$ and the gauge boson fusion processes $e^+e^- \rightarrow \nu\overline{\nu}H$ (WW fusion) and $e^+e^- \rightarrow e^+e^-H$ (ZZ fusion). The cross sections for these processes are shown in Fig. 2.14. With a typical integrated luminosity of 10 fb^{-1} at $\sqrt{s} = 500$ GeV with $M_H = 150$ GeV, about 1000 signal events would be expected before cuts and branching ratios. Handy "rules of thumb" are that the peak for ZH production occurs at $\sqrt{s} \approx M_Z + \sqrt{2}M_H$ and that the cross-over for equal cross sections from the fusion and bremsstrahlung mechanisms occurs at $\sqrt{s} \approx 0.6M_H + 400$ GeV.

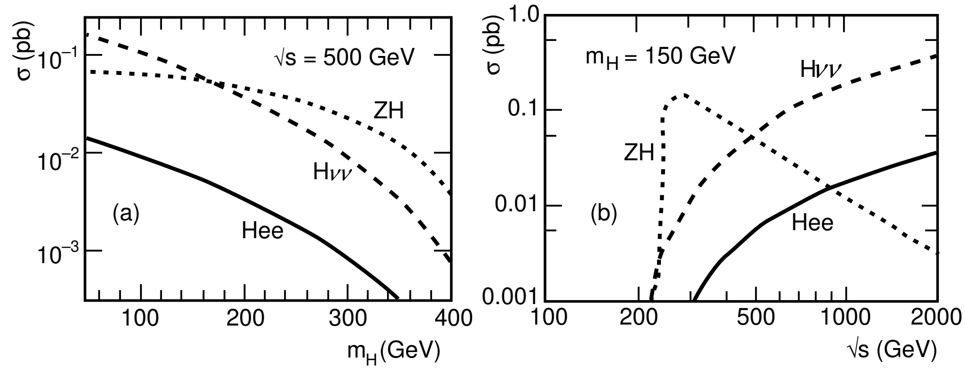

Figure 2.14: Cross section for Standard Model Higgs boson production.

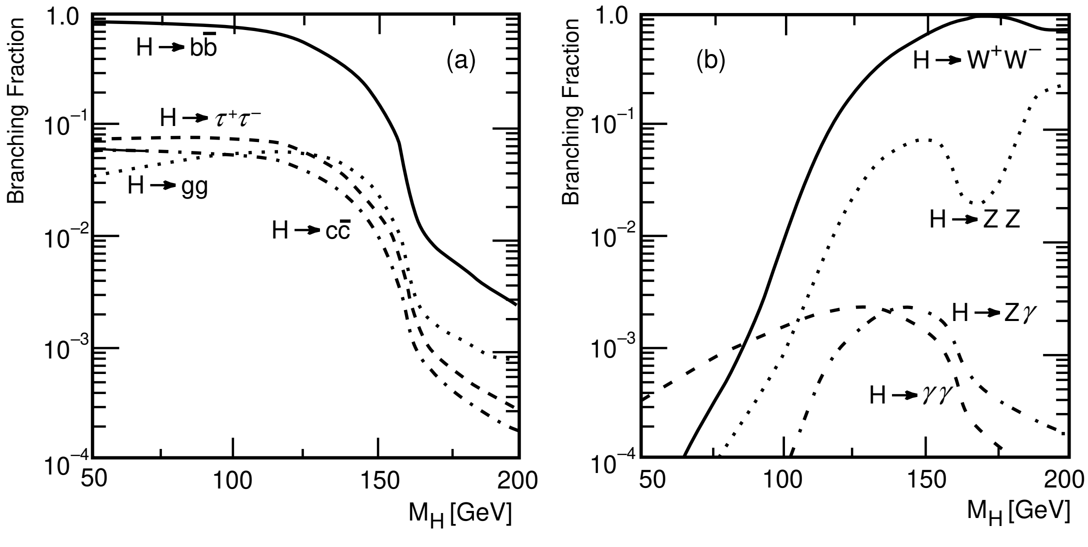

Figure 2.15: Branching fractions of a SM Higgs boson.

The decay modes of the Standard Model Higgs depend strongly upon its mass. The branching ratios of the Standard Model Higgs are shown in Fig. 2.15. A very interesting region is the intermediate mass Higgs with $M_Z < M_H < 2M_W$, which at a hadron collider is relatively more difficult to detect than a heavy Higgs boson. Almost all of the decays, both those to fermions and those into pairs of gauge bosons are identifiable in e^+e^- experiments, and it should be possible to measure individual branching ratios. For an intermediate mass Higgs, the dominant decay channel is clearly $H^0 \to b\overline{b}$, with the branching ratio for $H^0 \to W^+W^{-(*)}$ growing with increasing mass (even for $E_{cm} < 2M_W$ where one of the W's must be off shell). This latter channel remains dominant for heavy Higgs bosons, and is joined by ZZ and $t\overline{t}$ modes when kinematically accessible.

Signal Topologies and Backgrounds

Typical signal topologies in the intermediate mass range are shown in Fig. 2.16. The associated production $e^+e^- \to Z^0H^0$, is followed by standard decays of the Z^0 (10% $\ell^+\ell^-$, 20% $\nu\overline{\nu}$, and 70% $q\overline{q}$) and decays of the H^0 mostly into $b\overline{b}$, occasionally into $\tau^+\tau^-$, and more rarely into $c\overline{c}$ and gg. After straightforward cuts, the most serious backgrounds are due to irreducible Standard Model processes, $e^+e^- \to ZZ$, $Z\nu\overline{\nu}$, and $We\nu$.

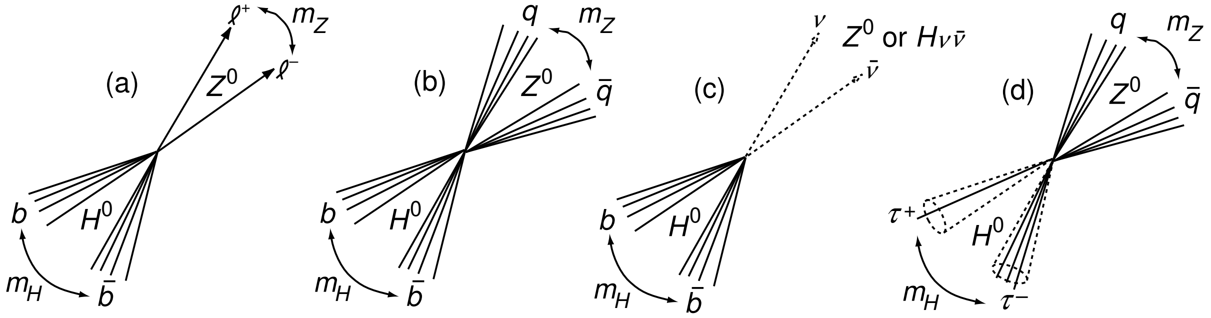

Figure 2.16: Important signal topologies for an intermediate mass SM Higgs boson.

Experimental Studies

The detection of Higgs bosons in e^+e^- collisions at high energy has been studied extensively in simulations [48, 45, 46]. The detector simulations that have been employed usually emulate LEP/SLC-type detectors using smeared four-vectors, while some consider simulations of a more ambitious JLC-type detector [47]. Most studies include the effects of beamstrahlung, the radiation of photons in the intense electromagnetic fields of the beam-beam collision. Like more standard initial-state radiation, this effect is usually taken into account in kinematic fits by allowing for an unknown missing momentum along the beam axis.

In the topology of Fig. 2.16a, one can first identify two leptons with invariant mass close to the mass of the Z^0, and then investigate the remaining hadronic mass or use kinematic constraints to study the missing or recoil mass in the event:

$$M_{miss} = \sqrt{(\sqrt{s} - E_{\ell^+} - E_{\ell^-})^2 - (\vec{p}_{\ell^+} + \vec{p}_{\ell^-})^2}.$$

This quantity has a large peak at the Z^0 mass from the irreducible background process $e^+e^- \to Z^0Z^0$; $Z^0 \to \ell^+\ell^-$; $Z^0 \to q\overline{q}$. If $M_H \approx M_Z$, the signal and the ZZ background are kinematically equivalent, and one would need b-quark tagging to distinguish the signal. Since $Br(Z^0 \to b\overline{b}) \simeq 20\%$, while $Br(H^0 \to b\overline{b}) \simeq 85\%$ at this mass, an analysis in this worst case would require 50 fb^{-1} of data.

The four-jet topology of Fig. 2.16b has been considered in a number of studies, in particular, in a comprehensive study by Janot [48] at $\sqrt{s} = 500$ GeV which assumed an integrated luminosity of 10 fb^{-1}. After selection cuts, for $M_H = 110$ GeV, a small signal is observed above the background, which comes mainly from $e^+e^- \to W^+W^-$, Z^0Z^0, and $qq(\gamma)$. This signal is greatly enhanced, as shown in Fig. 2.17b, by requiring that at least one of the jets forming the Higgs signal peak come from a tagged b quark. The vertex-tagger is assumed to have the conservative performance $\epsilon_{b\overline{b}} = 50\%$, $\epsilon_{c\overline{c}} = 2.5\%$, $\epsilon_{c\overline{s}} = 0.3\%$, and $\epsilon_{q\overline{q}} = 0.1\%$, where the numbers give the efficiency for tagging a particular quark combination. The importance of b tagging is even greater as one moves up in mass.

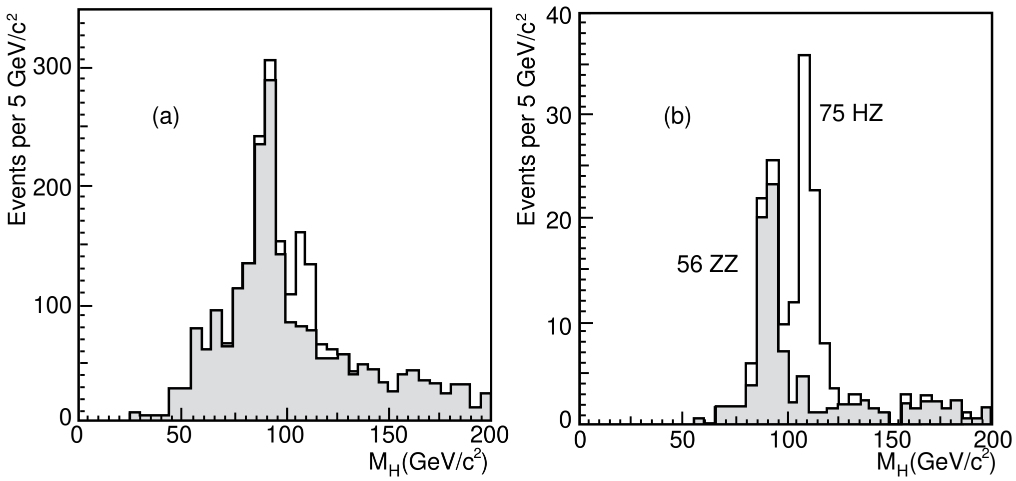

Figure 2.17: Distribution of the invariant mass of the Higgs jet pair in the four-jet topology (a) before and (b) after b-quark tagging, for all known backgrounds (shaded histograms) and for the signal ($M_H =$ 110 GeV) (adapted from Ref. 10).

The missing energy topology shown in Fig. 2.16c can arise either from the ZH process, with $(Z^0 \to \nu\overline{\nu})(H^0 \to b\overline{b})$, or from WW fusion. The resultant events will have large missing energy, transverse momentum, and mass, plus the presence of acoplanar jets. This distinctive signature offsets the loss of the Z-mass constraint. The last topology of Fig. 2.16d can be isolated by tagging two τ leptons either from their one- or three-prong decays recoiling against a reconstructed Z^0 decaying into $q\overline{q}$. Using a kinematically-constrained fit the missing neutrinos from the τ decay can be taken into account.

The examples given so far rely primarily on the large branching ratio for $H^0 \rightarrow b\overline{b}$. As the H^0 gets heavier, other decay modes begin to become important. For example, for $M_H = 140$ GeV, $Br(H^0 \rightarrow W^*W) \simeq 45\%$. The mode $(Z^0 \rightarrow q\overline{q})(H^0 \rightarrow W^*W)$ has been investigated [49] by demanding a six-jet event with a reconstructed Z^0 hadronic decay, one jet pair reconstructing to M_W, and the last pair peaking at $m < M_W$, depending on M_H. Similarly, for $M_H = 160$ GeV, the decay $H^0 \rightarrow W^+W^-$ dominates, and for production via fusion, $e^+e^- \rightarrow H\nu\overline{\nu}$, the result is an acoplanar pair of reconstructed W bosons and a total visible mass peaking at the H mass which is expected to be well above background without the need for b-tagging.

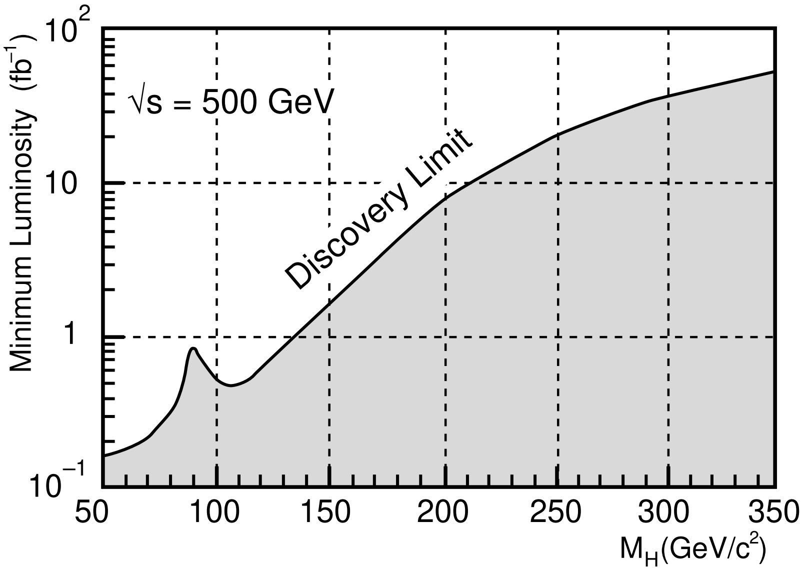

Figure 2.18: Minimum luminosity needed to discover a SM Higgs boson at a center-of-mass energy of 500 GeV.

Thus, studies have shown that with a detector similar to the LEP/SLC detectors, with b-quark vertex tagging provided by silicon microvertex detectors using present technology, an intermediate-mass SM Higgs boson cannot escape detection at an e^+e^- linear collider at $\sqrt{s} = 500$ GeV. Figure 2.18 shows an estimate [48] of the minimum luminosity required to discover at the 5σ level a SM Higgs boson of a particular mass. An integrated luminosity of only 5 fb^{-1} would be adequate to cover the entire intermediate mass range, while 20 fb^{-1} would allow a reach in mass up to about $\sqrt{s}/2$.

Higher $\sqrt{s}$ would of course allow one to probe for the existence of much heavier Higgs bosons, mostly through WW fusion and decay into pairs of vector bosons. At center of mass energies of 1–2 TeV, different backgrounds such as $e^+e^-W^+W^-$ and $e^+\nu_eW^-Z^0$ need to be addressed. Even though there exist older studies [7, 50] of searches for heavy Higgs bosons in 1–2 TeV e^+e^- collisions, these investigations need to be updated with more detailed simulations and to keep abreast of theoretical developments [51] regarding backgrounds and the decay of heavy Higgs bosons. For very large Higgs boson masses, this study becomes a part of the general problem of studying WW scattering at high energies; we discuss this problem in some detail in Section 7.2.

2.4.4 Minimal Supersymmetric Standard Model Higgs

In the framework of the MSSM, production of the lightest CP-even state h^0 is similar to that of the SM higgs boson. It is produced by the Zh and WW fusion processes just described, with h^0 replacing h_{SM}. In addition, new modes of production also open up, involving the heavy Higgs bosons H^0 and A^0. The various production processes for h^0 and H^0 in e^+e^- annihilation depend on the mixing angles α and β as indicated in Table 2.5. Notice the sum rule: One process in each line always has a substantial rate. As $m_A \to \infty$ in the MSSM, $\cos(\beta - \alpha) \to 0$, and only the processes in the left-hand column of the table occur. In this limit, the rates of the h^0 production processes are identical to those for the Standard Model Higgs.

Table 2.5: Dependence of the cross section on Higgs boson mixing angles for various Higgs boson production processes in the MSSM.

$\sin^2(\beta-\alpha)$	$\cos^2(\beta-\alpha)$
h^0Z^0	H^0Z^0
$h^0\nu\overline{\nu}$	$H^0\nu\overline{\nu}$
H^0A^0	h^0A^0

The phenomenology of the SUSY Higgs bosons varies in a smooth way as M_A is varied. The contours of Higgs mass over the MSSM parameter space are shown in Fig. 2.19 [52]. If $M_A < 125$ GeV, then A^0 and h^0 are close in mass; if $M_A > 125$ GeV, then $M_A \simeq M_H$ and we begin to approach the large M_A limit. However, if $M_A < 230$ GeV, then all of the MSSM Higgs bosons should still be observable at the NLC with $\sqrt{s} = 500$ GeV. If $M_A > 230$ GeV, it is possible that, at the $\sqrt{s} = 500$ GeV stage of the NLC, only the lightest SUSY Higgs h^0 may be observable *and* it would have production rates virtually indistinguishable from those of a minimal Standard Model Higgs boson. The remaining Higgs states could be discovered at higher $\sqrt{s}$, and there are also precision tests available, to be described later, which could distinguish a Standard Model Higgs from a supersymmetric Higgs. However, since the h^0 will result in decay topologies similar to that of the SM Higgs, if this lightest h^0 is not observed, then the MSSM is categorically ruled out. If the h^0 is not seen below 150 GeV, the more general supersymmetry models incorporating grand unification are also excluded.

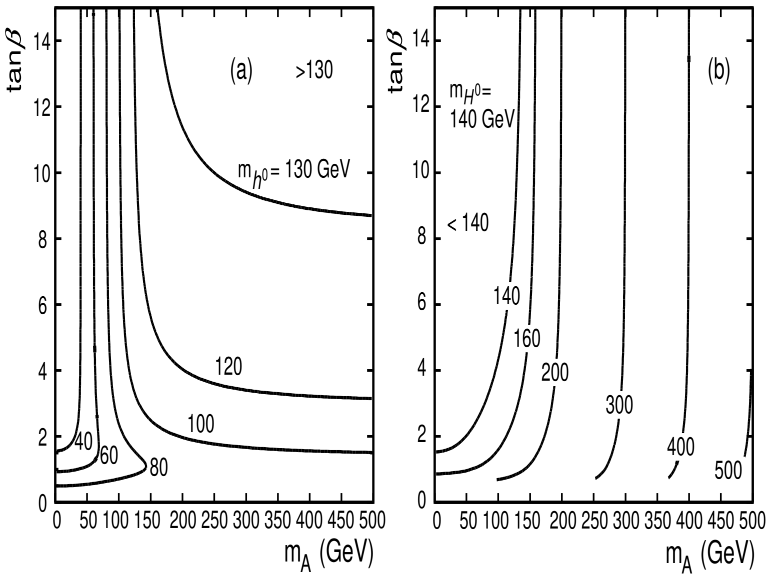

Figure 2.19: Contours of the values of (a) M_h and (b) M_H in the MSSM for $m_t = 180$ GeV, assuming $m_{SUSY} = 1$ TeV and maximal top squark mixing.

In general, for an intermediate mass boson, the branching ratio for a minimal SM Higgs boson to $b\bar{b}$ is very close to that of the light CP-even state h^0. For large values of $\tan\beta$, the other neutral MSSM Higgs bosons decay predominantly into $b\bar{b}$, with a 3% branching ratio into $\tau^+\tau^-$. This simple pattern becomes more complex for smaller values of $\tan\beta$ [51] with modes such as $H^0, A^0 \to t\bar{t}$ (for $M_{A^0} \approx M_{H^0} > 2m_t$) and $H^0 \to h^0h^0$ and $A^0 \to Zh^0$ (for $M_{A^0} \approx M_{H^0} < 2m_t$) becoming more important. Despite more complicated cascade decays into lighter Higgs states, the bottom line remains clear: There should be plenty of jets from b-quarks to tag and elucidate signals. A case in point is the spectacular decay of H^0A^0 into six b jets $H^0 \to h^0h^0$, $h^0 \to b\bar{b}$. Most final states decay into at least four b-quark jets, underlining the overwhelming importance of b-tagging in experimental studies. An interesting case deserving further study in simulations is the heavy Higgs decay into $t\bar{t}^{(*)}$.

Experimental Studies

All of the topologies of Fig. 2.16 can be explored in the MSSM with the h^0 taking the role of the Standard Model Higgs boson. A repetition of the analyses described earlier either would observe a single h^0 similar to that of the SM Higgs, or, if $\sin^2(\beta - \alpha) \simeq 0.5$, would observe both the h^0 and H^0 states as shown in Fig. 2.20a [48].

An identical preselection for a four-jet topology can be used to search for HA. We require in this case that all four jets in $(H^0 \to b\bar{b})(A^0 \to b\bar{b})$ be tagged as b jets. For large enough M_A and $\tan\beta$, we have $M_A \simeq M_H$, and we can demand that the two jet-pair masses of the

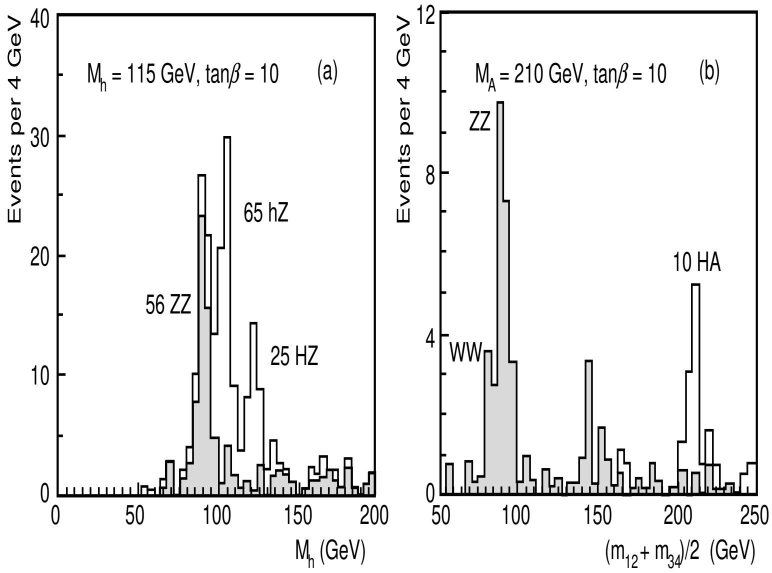

Figure 2.20: (a) Jet masses recoiling from a reconstructed Z^0 after b tagging for $\sin^2(\beta-\alpha) \simeq 0.5$, and integrated luminosity of 10^{-1} fb; (b) average of the two jet-pairs closest in invariant mass in an identified $b\overline{b}b\overline{b}$ final state with $M_A = 210$ GeV (adapted from [48]).

possible combinations to be close to equal. Then a signal as shown in Fig. 2.20b is possible. Since all the neutral SUSY Higgs decay into $\tau^+\tau^-$ at some level, it is possible to observe all three MSSM states in a single analysis by looking at the invariant mass of both the $\tau^+\tau^-$ and $q\overline{q}$ in the $\tau^+\tau^- q\overline{q}$ final state. In Fig. 2.21, we show the regions of plane of M_A versus M_h in which is it possible to observe all three neutral Higgs states of the MSSM at a linear collider with $\sqrt{s} = 500$ GeV, or, conversely, the region where only the h^0 can be observed [53].

In theories with multiple Higgs doublets such as the MSSM, searches for the charged Higgs bosons $H^\pm$ are also important. An e^+e^- collider should be able to better resolve the hadronic decays of the $H^\pm$ compared to a hadronic collider, and all of the expected final states $H^+H^- \to c\overline{s}\,\overline{c}s$, $t\overline{b}\overline{t}b$, plus the easier topologies of $c\overline{s}\tau^-\nu$ and $\tau^+\nu\tau^-\overline{\nu}$ should be observable. A detailed simulation analysis [54] at $\sqrt{s} = 500$ GeV with an integrated luminosity of 10 fb^{-1}, which makes heavy uses of b-tagging, has shown that one can establish a signal over the $e^+e^- \to t\overline{t}$ and W^+W^- background in all of these channels. The results show a detection sensitivity for charged Higgs bosons up to about 210 GeV at $\sqrt{s} = 500$ GeV, independent of decay mode. These conclusions can be strengthened further by adding the decay $t \to bH^+$. The bottom line is that if the A^0 is lighter than about 200 GeV, then the $H^\pm$ should be observable also.

If one is considering SUSY Higgs bosons, one should allow for the possibility of their decay into other SUSY particles. As an example, it is possible for h^0 or H^0 to decay into a pair of the lightest neutralinos (mixtures of fermionic partners of the Z and γ) that would be stable and neutral. The result would be an "invisible" decay of the Higgs. This topology

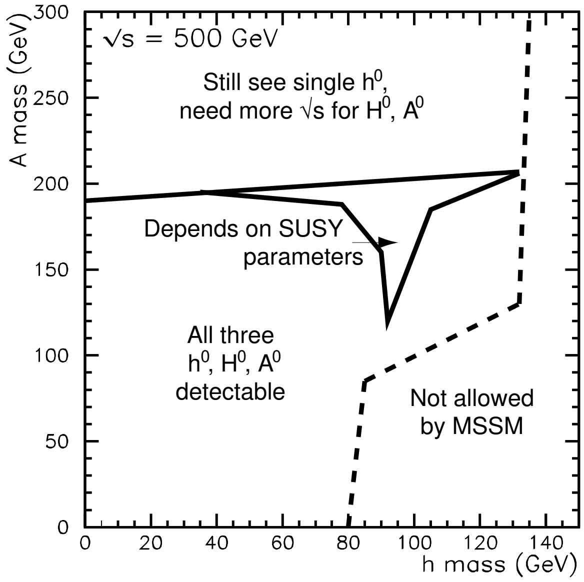

Figure 2.21: Regions of simultaneous detectability of h^0, H^0, and A^0 at center-of-mass energy of 500 GeV [53].

can be identified in the same way as described previously by studying the missing mass in a hZ or HZ event where the Z decays into a pair of electrons or muons. Both missing mass resolution and backgrounds (smaller direct $Z\nu\overline{\nu}$ cross section) improve with lower center-of-mass energy, and such an analysis would benefit from running at $\sqrt{s} \simeq 300$ GeV. The possibility of SUSY Higgs decays into other SUSY particles [51] such as SUSY partners of quarks and leptons warrant further experimental simulations.

2.4.5 Determination of Properties of Higgs Bosons

Mass Measurement

To measure the mass of one or more of the possible Higgs bosons, one would probably optimize the running conditions to have smaller center-of-mass energy , to improve momentum resolution and to go to the peak of the cross section. For an intermediate mass Higgs, $\sqrt{s} = 200$–300 GeV is appropriate. Under these conditions, one can precisely measure the recoil mass in $e^+e^- \to Z^0h^0$ events opposite to the reconstructed leptonic decay $Z^0 \to e^+e^-$ or $\mu^+\mu^-$. Other modes, such as the four-jet topology, can also be employed. In all cases, kinematic fitting would be used to constrain the leptons or jets from a Z^0 to reconstruct to M_Z and to allow for missing E_γ along the beam axis. A typical jet-jet mass resolution of $\sigma_M \simeq 2.0$ GeV can be achieved assuming the excellent momentum resolution of $\sigma_{p_t}/p_t = 1 \times 10^{-4} \oplus 0.1\%$ envisaged for the JLC detector [47]. For our NLC detector design, we could achieve $\sigma_M \simeq 3.9$ GeV, as shown in Fig. 2.22. The differences between detector designs are much smaller when kinematic constrained fitting is included in the analysis. The

JLC-type detector has been estimated to provide a estimated precision on the Higgs mass of approximately 0.1% for $\sqrt{s} = 300$ GeV, $\int L \cdot dt = 30$ fb^{-1}, and a 2.0% full width beam energy spread [55]. On the other hand, the NLC-type detector gives $\Delta M_h \leq 160$ MeV up to $M_h \simeq 160$ GeV with 50 fb^{-1} at $\sqrt{s} = 500$ GeV.

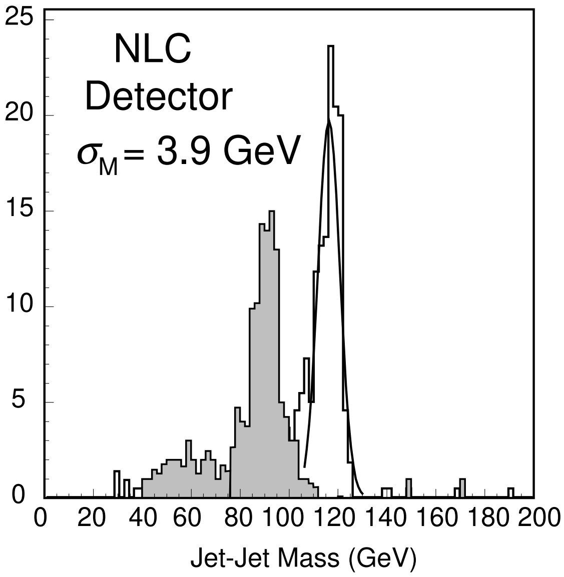

Figure 2.22: Mass resolution of $\sigma_M \simeq 3.9$ GeV in the jet-jet invariant mass for jets from Higgs decay assuming the performance of a NLC detector (see text) for a simulated signal (open histogram) of a 120 GeV SM Higgs boson and all known backgrounds (shaded histogram) at 300 GeV with 10 fb^{-1}.

Once M_H is known precisely, it can be used as an input to check the experimental measurements of branching ratios and the production cross section with Standard Model predictions. Its value can also be compared to the theoretical value obtained from precision electroweak measurements, combined with the measurements of M_W and m_{top} expected from a linear collider.

Cross Section Measurement

Measuring the production cross section of the Higgs provides one way of disentangling a SM Higgs boson from a SUSY Higgs, if one can observe the cross section suppression due to mixing

$$\sigma(e^+e^- \to h^0 Z^0) = \sin^2(\beta - \alpha) \cdot \sigma(e^+e^- \to h^0_{SM} Z^0).$$

A distinct advantage of e^+e^- linear colliders over hadronic colliders is the ability to almost unambiguously tag the Z^0 in hZ events and being able to study all of the decays $h^0 \to X$ with small backgrounds. Both total absolute cross sections and individual Higgs branching ratios can then be measured. By using leptonic decays of the Z^0 and kinematical fitting, the absolute production cross section can be measured [55] with a precision of 7% with an integrated luminosity of 30 fb^{-1} and to 5% with 50 fb^{-1}. However it should be kept in mind that for a large area of SUSY parameter space, the SUSY Higgs cross section is less than 10% different from the SM Higgs cross section.

Spin-Parity and CP Determination

In principle, the spin and parity of the Higgs boson can be found by studying both the production angular distribution of the Higgs and also the resulting angular distribution of the decay products of the Z^0 in its rest frame in HZ events. In the high energy limit, Table 2.6 shows the expected angular distribution of scalar (*e.g.*, h^0, H^0) and pseudoscalar (*e.g.*, A^0) Higgs bosons. In the table, θ is the production angle of the Higgs boson and θ_* is the polar angle of the fermions from Z decay measured in the Z rest frame. In practice, however, a purely CP-odd Higgs boson couples to ZZ only at the one-loop level, and then the ZA cross section would be very small. For a Higgs boson that is a mixture of CP-even and CP-odd components, the production would mainly be sensitive to the CP-even part, and the angular distributions would not reveal the CP-odd component [56].

Table 2.6: Expected angular distributions for Higgs bosons with different spin-parity.

	Scalar, 0^{++}	Pseudoscalar, 0^{-+}
$d\sigma(e^+e^- \to HZ^0)/d\cos\theta$	$\propto \sin^2\theta$	$\propto (1-\sin^2\theta)$
$d\sigma(Z^0 \to f\overline{f})/d\cos\theta_*$	$\propto \sin^2\theta_*$	$\propto (1 \pm \cos\theta_*)^2$

A much better way to determine the Higgs' CP character is with polarized $\gamma\gamma$ collisions [57, 58]. In this technique, which we will discuss in detail in Section 9.2, the Higgs boson is produced as an s-channel resonance. Then it is possible to study the angular correlations of the decay products of the resonance in decays such as $H \to \tau^+\tau^-$ and $t\overline{t}$. By spin analyzing the subsequent decays $t \to b\ell\nu$ for top quarks from heavy Higgs boson decay, and $\tau \to \pi\nu$ or $\tau \to \rho\nu$ for τ's from intermediate mass Higgs decay, a CP-even state and CP-odd state can be distinguished [56, 59]. This CP state separation is much better in the angular correlations between top quark decay products.

Branching Ratio Measurements

The measurement of the branching ratios of any observed Higgs boson is an essential ingredient to understand the nature of the symmetry breaking and to make predictions about other aspects of the Higgs sector. This is especially when only a single neutral Higgs is observed, which might be either the Standard Model Higgs or the lightest neutral Higgs from SUSY.

The clean environment in e^+e^- annihilation permits one to tag a Z^0 in one hemisphere, and then observe the decay $h^0 \to X$ in any decay mode in the opposite hemisphere. An example of such an analysis [49] at $\sqrt{s} = 400$ GeV, simulating an SLD-like detector, first identifies a Z^0 in a HZ event and then considers those decays where the recoiling Higgs decays into jets. The Higgs decays to two jets can be separated by flavor by counting the number of tracks with a significantly large impact parameter: $b_{norm} = b/\sigma_b > 3$, where b is the impact parameter and σ_b is the error on b. The decay $h \to WW^{(*)}$ is identified by demanding that the event be consistent with containing six jets, and that a jet pair with invariant mass close to the W mass is found. With 50 fb^{-1} of data, $Br(h \to b\bar{b})$ can be measured to a statistical precision of 7%, and branching ratios into WW^* and $(c\bar{c} + gg)$ to 24% and 39% respectively. These relative errors are shown superimposed upon the Standard Model values in Fig. 2.23a. The figures also shows the variation in branching ratios that one would expect from the variation of $\tan\beta$. In the MSSM, it is very difficult to arrange such a large variation in $\tan\beta$ without a compensatory variation in α, but the figure shows the utility of this measurement in Higgs studies in a more general context. For the comparison of the Standard Model Higgs boson to the MSSM, one should consult Fig. 2.23b, where the branching ratio of a light Higgs boson into $b\bar{b}$ is compared for these two possibilities over the MSSM parameter space.

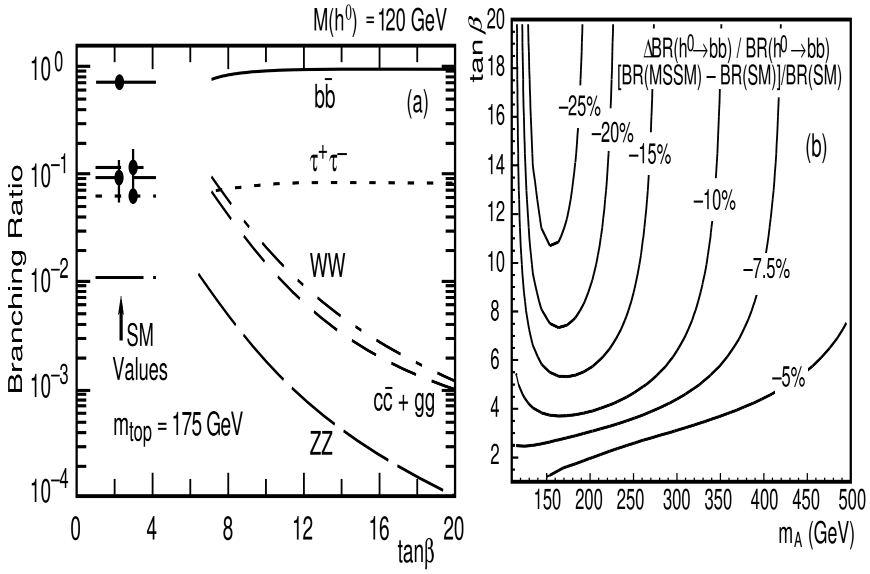

Figure 2.23: (a) Expected errors on the Standard Model branching fractions compared to those predicted for a 120 GeV h^0 MSSM Higgs boson; (b) contour lines of fractional deviation of $Br(h^0 \to b\bar{b})$ ($m_t =$ 175 GeV, $m_{SUSY} = 1$ TeV).

An interesting quantity [61] is the ratio of branching ratios to $c\bar{c}$ versus $b\bar{b}$. At tree level,

$$\frac{Br(h \to c\bar{c})}{Br(h \to b\bar{b})} \approx \frac{m_c^2}{m_b^2} \cdot \left(\frac{M_h^2 - M_A^2}{M_A^2 - M_Z^2} \right)^2 ,$$

where m_c and m_b are the c and b quark masses respectively. (We should note that this formula can receive substantial radiative corrections in some regions of the MSSM parameter space.) If the branching ratios indicated are measured along with M_h, it is possible to estimate M_A. In a simulation study of this measurement [62] at $\sqrt{s} = 300$ GeV, HZ events are selected for each decay mode of the Z^0, and the decay mode of the Higgs is determined using three-dimensional impact parameters. Flavor tagging is performed by selecting charged tracks that satisfy $b/\sigma_b \geq 2.5$ and counting the number in each jet from the Higgs decay. For $M_H = 120$ GeV, 50 fb^{-1} of data, and assuming 90% polarization of the electron beam, the statistical error on the ratio of branching ratios $Br(h \to c\bar{c}+gg)/Br(h \to b\bar{b})$ would be 20.4%, varying with the Higgs mass as shown in Fig. 2.24a. This does not include a substantial systematic uncertainty from m_c/m_b, which we believe will be reduced in the next few years through lattice gauge theory calculations. Then, as shown in Fig. 2.24b, this measurement could be sensitive to A^0 masses up to 400 GeV, well above the maximum kinematic reach of a 500 GeV collider. Observation of the A^0 in this way would help to plan the next step in energy.

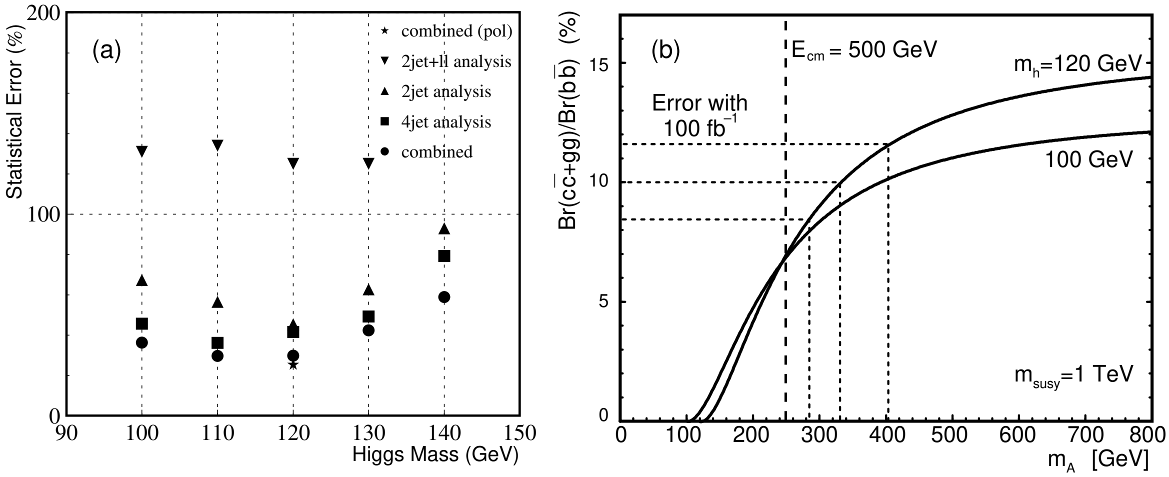

Figure 2.24: (a) Statistical error with 50 fb^{-1} of data on $Br(h \to c\bar{c} + gg)/Br(h \to b\bar{b})$ as a function of Higgs mass; (b) implications for estimation of A^0 mass.

For the decay $h \to \gamma\gamma$, it is difficult to measure the branching ratio at an e^+e^- collider because this mode is relatively rare. However, it should be possible to measure the absolute partial width $\Gamma(h \to \gamma\gamma)$ by exploiting the ability of an electron collider to be run as a $\gamma\gamma$ collider. This measurement is discussed in Section 9.1.

Determination of Higgs Total Width

In the preceding sections, we have indicated many ways in which measurements at the NLC can distinguish between the Standard Model Higgs and the light Higgs h^0 of the MSSM. There are also a number of quantities at the LHC which are sensitive to this difference, as outlined in [35]. However, to obtain the complete set of partial width of the Higgs boson in a model-independent way, measurements from LHC must be combined it with data both from e^+e^- and $\gamma\gamma$ collisions at the NLC. A possible procedure is the following. First determine $Br(b\bar{b})$ from Zh events and combine with $\sigma(WW \to h) \cdot Br(b\bar{b})$ both measured at the NLC to obtain the WWh coupling. Alternatively, a measurement of $\sigma(e^+e^- \to Zh)$ at the NLC gives the ZZH coupling and the ratio of the WWh and ZZh couplings given by $M_W^2/M_Z^2 = \cos^2\theta_W$ also gives the WWh coupling. This coupling and a measurement of $\sigma(Wh) \cdot Br(\gamma\gamma)$ at the LHC can be used to determine $Br(\gamma\gamma)$. Therefore one can combine $Br(b\bar{b})$ with the $\gamma\gamma$ collider measurement of $\sigma(\gamma\gamma \to h) \cdot Br(b\bar{b})$ to obtain $\Gamma(h \to \gamma\gamma)$. We can then finally compute the total width $\Gamma_h^{\rm tot} = \Gamma(h \to \gamma\gamma)/Br(\gamma\gamma)$ and $\Gamma(h \to b\bar{b}) = Br(b\bar{b})\Gamma_h^{\rm tot}$. A simpler route exists using only e^+e^- data when the Higgs boson is heavy enough that the branching ratio to WW^* is relatively large, so that it can be measured accurately. In this case, we can simply measure $Br(h \to WW^*)$ and infer $\Gamma_h^{\rm tot} = \Gamma(h \to WW^{(*)})/Br(WW^{(*)})$. Although the accumulation of errors may be significant, the basic point is that data from all three colliders or from the NLC alone can be combined to complete a *model-independent* determination of the properties of a light Higgs boson.

2.4.6 Summary

From the studies described, the discovery of a Standard Model intermediate-mass Higgs boson at an e^+e^- linear collider at $\sqrt{s} = 500$ GeV can be easily achieved with an integrated luminosity of only 10 fb^{-1}. Such a machine allows the detection of *at least* the lightest MSSM Higgs h^0, if not all three SUSY neutral states. If the lightest Higgs is not observed, then not only is the Minimal Supersymmetric Standard Model ruled out, but also the general idea that the Higgs boson is a fundamental particle up to the unification scale is called into question. If the A^0 is not kinematically accessible at $\sqrt{s} = 500$ GeV, then the measurement of h^0 branching ratios can give hints of the values of M_A and $\tan\beta$ and tell us where to go next in energy. For definitive evidence, $\sqrt{s} > 2M_A$ would still be needed. For Higgs bosons above the intermediate mass range, their decay into pairs of vector bosons makes them straightforward to detect at the NLC as at the LHC; however, more up-to-date experimental simulations are needed. Just as important as its ability to discover the Higgs boson is the ability of the linear collider to make precision measurements of the properties and couplings of a Higgs boson. Even if the Higgs boson is discovered earlier at LEP2 or at the LHC, we will need the NLC to learn its complete story.